Desalination 520 (2021) 115368

Contents lists available at ScienceDirect

Desalination

journal homepage: www.elsevier.com/locate/desal

Block copolymer coated carbon nanotube membrane anodes for enhanced and multipurpose hybrid capacitive deionization

Sen Xiong, Li Ren, Chenxu Zhang, Jiemei Zhou, Yong Wang *

State Key Laboratory of Materials-Oriented Chemical Engineering, College of Chemical Engineering, Nanjing Tech University, Nanjing 211816, Jiangsu, PR China

HIGHLIGHTS

- The BCPs and selective swelling are introduced to fabricate CDI electrodes.
- The protonated blocks in BCP make the electrodes especially suitable for anodes.
- The CDI performance of CNT membranes is significantly improved by this method.
- The module type and initial solution pH have marked influence on the CDI performance.
- The hybrid CDI module exhibits promoted adsorption towards different anions.

GRAPHICAL ABSTRACT

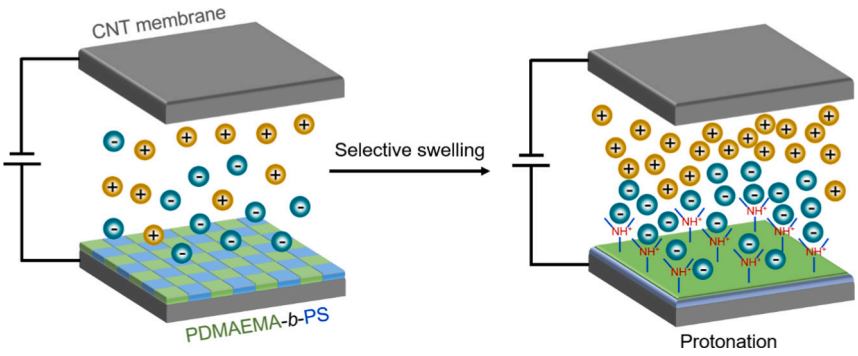

ARTICLE INFO

Keywords:
Hybrid capacitive deionization
Carbon nanotube membranes
Anode production
Block copolymer
Selective swelling

ABSTRACT

Carbon nanotube (CNT) membranes are widely used electrode materials in capacitive deionization (CDI) processes, while the limited electrosorption capacity and poor long-term stability need to improve. In this work, a pH-responsive block copolymer (BCP), poly (2-dimethylaminoethyl methacrylate)-*block*-polystyrene (PDMAEMA-*b*-PS) is combined with the selective swelling to fabricate a CNT membrane based multipurpose electrode. After BCP coating and selective swelling, the PDMAEMA blocks migrate onto the membrane surface and protonate during the CDI processes, which enhance the attraction between electrode and anions. Therefore, the BCP coated electrodes can be used as high performance anodes in the hybrid CDI (HCDI) module. Experiment results show that the initial solution pH values have significant influence on the CDI performance of the HCDI module. The maximum removal efficiencies of the HCDI module towards NaCl and NaH_2PO_4 are ~15 mg·g^{-1} and ~38.7 mg·g^{-1}, respectively. Moreover, the chemical and mechanical stabilities of the anodes are significantly enhanced. No anode oxidation can be observed during CDI processes and the frequently occurred co-ion repulsion effect is suppressed. Considering these advantages, the combination of BCPs and selective swelling will be a promising candidate for the development of HCDI module.

* Corresponding author.
E-mail address: yongwang@njtech.edu.cn (Y. Wang).

https://doi.org/10.1016/j.desal.2021.115368
Received 19 July 2021; Received in revised form 9 September 2021; Accepted 20 September 2021
Available online 25 September 2021

1. Introduction

With the rapid growth of human society, demands on fresh water have grown enormously. Membrane separations and thermal separations are frequently used to desalinate seawaters and brackish waters to acquire fresh water. However, all these methods require massive energy to generate driving forces to complete the separation. Capacitive deionization (CDI) is an emerging electrochemical desalination technology, which can separate the salts from solutions by adsorbing anions and cations onto anodes and cathodes, respectively [1,2]. Comparing with the pressure- or thermal-driven desalination processes, the CDI process is independent of the expensive and energy-intensive equipment. Moreover, the voltage applied in CDI is generally lower than the water redox potential, thus the energy consumption and safety of CDI processes are better than other desalination methods [3].

The performance of CDI processes is determined by the electrode materials and module types. Due to the high porous structure and excellent conductivity, carbon-based materials, from the commonest activated carbons (ACs) to the widely studied carbon nanotube (CNT), have been introduced into the CDI as electrodes and greatly promote the development of CDI processes [1,4]. There are two electrochemical mechanisms working during the CDI processes, i.e. the electric double layer (EDL) adsorption and Faradaic ion storage [5,6]. The EDL-based adsorption is originated from the potential difference applied on the electrodes. During the adsorption process, the cations and anions are immigrated to the double layers around the surface of cathode and anode, respectively [5]. For Faradaic ion storage, the ions are stored around the electrode surface through reversible redox reactions [6]. However, the electrodes based on EDL adsorption are facing the co-ion expulsion effect and the carbon materials at anodes will be oxidized in long-term use [7,8].

To solve these problems, researchers propose many solutions to design new CDI modules, such as membrane capacitive deionization (MCDI) [9–11], flow-electrode capacitive deionization (FCDI) [12,13], and batteries CDI [14,15]. Among all these methods, Lee et al. [16] constructed a hybrid CDI (HCDI) module, which applied EDL adsorption on one electrode and Faradaic reaction on the other. With the help of Faradaic reaction, the electrosorption capacity of the HCDI module is improved and the co-ion expulsion effect has been greatly alleviated. However, the majority of researches on HCDI module are concentrated on the modification of cathodes. $Na_4Ti_9O_{20}$ [17], MXene [18], $Na_2FeP_2O_7$ [19], redox-active polyimide [20], covalent organic frameworks [21], and many other materials have been successfully used as cathodes in HCDI. Researchers find that adding anion exchange membranes will significantly enhance the performance and stability of CDI modules [22,23], while the complexity as well as the operation costs of CDI modules are increasing. Interestingly, researchers also confirm that the cathodes show low demands on the ion-exchange membranes [24]. Therefore, modifications on anodes may free the HCDI modules from ion-exchange membranes and simplify the whole system.

Ag and BiOCl are widely used anion storage materials [25–27], while these materials are exclusively on the adsorbing of chloride ions. To expand the application of modified anodes, conductive polymers containing nitrogen element are introduced into the fabrication of electrodes, which can enhance the conductivity, avoid raw material agglomeration, and protect the carbon materials [28]. Liu et al. [29] added an anionic polymer (with trimethylamine functional groups) on the carbon cloth and then used the composites as CDI anodes. After introducing as-prepared anodes, the CDI processes showed better salt removal efficiency and the anionic polymer protected the carbonic anodes from oxidation. Other materials, such as polypyrrole [30] and polyaniline [31,32], are also applied in the modification of anodes. Zhao et al. [33] doped chloride into polypyrrole (PPyCl) and then mixed the PPyCl with CNTs to fabricate PPyCl@CNT anodes. The CDI module using PPyCl@CNT anodes exhibited excellent reusability, which could adsorb and desorb ions from NaCl solution reversibly for 200 cycles. In recent years, researchers found that, after introducing pH-responsive polymers into CDI processes, the ions adsorption could be enhanced by the electrostatic attraction between the polymers and ions. By grafted methacrylamide (MAAm) and 2-(dimethylamino)ethyl methacrylate (DMAEMA) onto polyethylene (PE), Kitao et al. prepared a pH-responsive polymer (PE-g-PMAAm)-g-PDMAEMA [34]. The PDMAEMA blocks would be protonated when the pH lower than 7.4 [35]. The protonated dimethylamine groups on the polymer backbone could adsorb negatively charged Cr(VI) ions from the solution by electrostatic interaction.

Based on our previous works, the CNT membranes have been confirmed to be excellent substrates in water treatments and CDI processes [36–38]. Therefore, combining with the researches mentioned above, we design a CNT membrane based HCDI module at the aim of combining the advantages of EDL adsorption and Faradaic ion storage mechanisms. A pH-responsive block copolymer (BCP), (2-dimethylaminoethyl methacrylate)-*block*-polystyrene (PDMAEMA-*b*-PS), is coated onto CNT membranes followed by selective swelling to fabricate Faradaic anodes. After selective swelling, the PDMAEMA blocks are migrated to the membrane surface and protonated in acidic solutions. With the increasing of solution acidity, the electrosorption capacity of the HCDI module towards different salts promotes significantly, and the initial pH value of the solution has obvious influence on the performance of the HCDI module. The strong π-π interaction between the CNT membranes and PS blocks of the BCP gives the modified anodes excellent mechanical stability. Moreover, the swollen BCP layers can protect the CNT membranes anodes from oxidation and co-ion expulsion effect. By optimizing the preparation parameters, the HCDI module exhibits desirable removal efficiency towards NaCl solutions as well as simulated phosphorous wastewaters. In this work, we present advantages of introducing the combination of pH-responsive BCP and selective swelling into CDI electrode fabrication processes, and we hope this work will extend the application of both BCPs and electrochemical desalination.

2. Experimental

2.1. Materials

The free-standing multiwalled carbon nanotube (CNT) membranes were bought from Suzhou Jiedi Nanotechnology Co., Ltd. The synthesis of poly (2-dimethylaminoethyl methacrylate)-*block*-polystyrene (PDMAEMA-*b*-PS, $M_n^{PDMAEMA}$ = 21.5 KDa, M_n^{PS} = 70.1 KDa, PDI = 1.16) was consistent with our previous work [39]. Anhydrous ethanol was purchased from Shanghai Aladdin Biochemical Technology Co., Ltd. Chloroform was acquired from Sinopharm Chemical Reagent Co., Ltd. Sodium dihydrogen phosphate, sodium hydroxide, hydrochloric acid, and deionized water were obtained from local suppliers.

2.2. Electrode preparation

A certain amount of PDMAEMA-*b*-PS was weighed and dissolved in chloroform to form solutions with concentrations of 1 wt%, 2 wt%, and 5 wt%, respectively. All solutions were filtered by polytetrafluoroethylene (PTFE) filters (0.22 μm) for three times to remove possible impurities. The CNT membranes were cut into 5 × 5 cm^2 and washed by anhydrous ethanol for several times, then stored in deionized water tanks before use. For cathodes, the CNT membranes were took out from the deionized water followed by a drying process and directly used as electrodes. For anodes, the CNT membranes were took out and put on a glass plate. The excessive water on the membrane surface was removed by dustless papers. Then 600 μL PDMAEMA-*b*-PS solution with different concentrations was spin-coated (100 rpm) onto the CNT membranes. Subsequently, the spin-coated CNT membranes were dried in an oven under 60 °C for 20 min to remove the organic solvent. The dried composite membranes were soaked in the ethanol solution and heated under 60 °C with chosen times to complete the selective swelling process. To

investigate the influence of swelling time, the samples with (5 h and 10 h) and without (0 h) selective swelling processes were prepared. Finally, the CNT membranes were dried at room temperature and then used as anodes in the HCDI module. As shown in Scheme 1, the strong π-π interaction between CNTs and PS blocks of the BCP endows the anodes with excellent mechanical stability [40]. While the protonated dimethylamine groups (-N(CH_3)$_2$) in PDMAEMA blocks provide high charge density to selectively adsorb anions from solution. Corresponding anodes were denoted as CNT membrane electrode-*w*/*t* (CME-*w*/*t*, *w* represented the concentration of spin-coating solutions, *t* represented the swelling times).

2.3. Characterization

The morphologies of all samples were characterized by a field-emission scanning electron microscope (FESEM, Hitachi, S4800) under the accelerating voltage of 3 kV. A layer of platinum was sputtering coated onto all samples before testing. To further investigate the structure change of CNT membranes and CMEs, a high resolution transmission electron microscope (HRTEM, JEOL, JEM-2100) was employed to study the influence of BCP coating. Fourier transform infrared spectroscopy (FTIR, Thermo Scientific, Nicolet 8700) was applied to analyze the chemical composition difference between the CNT membranes and CMEs under attenuated total reflectance mode. To examine the movement of PDMAEMA blocks induced by the selective swelling process, X-ray photoelectron spectroscopy (XPS, Thermo Scientific, K-alph) was adopted to analyze the N element content on the sample surface. The wettability of CNT membranes and CMEs were evaluated by the static water contact angles (WCAs) measured on a contact angle goniometer (Maist, Dropmeter A100).

2.4. Electrochemical property and CDI performance tests

The electrochemical properties of each sample were characterized by an electrochemical workstation (Shanghai Chenhua, CHI660E) in the conventional three-electrode cell and a NaCl solution (1 mol·L^{-1}) was used as the electrolyte. During the test, the Ag/AgCl electrode, platinum wire, and testing samples were employed as reference electrode, counter electrode, and working electrodes, respectively. The cyclic voltammetry (CV) curves were carried out with a scan rate of 10 mV·s^{-1} within the potential range between −0.8 V to 0.4 V. Electrochemical impedance spectroscopy (EIS) of each sample was conducted from 1 to 100,000 Hz with an oscillation amplitude of 5 mV.

The CDI performance of all electrodes was tested on a homemade apparatus [37]. To determine the influence of BCP concentration and swelling time on the CDI performance, the CMEs and pristine CNT membranes were comprised HCDI modules and used to desalt a testing solution. During the testing, 40 mL NaCl solution with a concentration of 100 mg·L^{-1} was used. All NaCl testing solutions were prepared by the deionized water with a pH value of 6.31 unless otherwise stated. After determining optimized preparation conditions, the selected samples were tested with 40 mL solutions with different NaCl concentrations and pH values (adjusted by HCl or NaOH), which could study the influence of treated solutions on the electrosorption capacity of the HCDI module. To further investigate the phosphorus removal efficiency, the HCDI module with different CMEs was used to deionize NaH_2PO_4 solutions (25 mL, 300 mg·L^{-1}). The phosphorus removal efficiency was measured by an inductively coupled plasma-optical emission spectrometer (ICP, PerkinElmer, Optima 7000DV).

3. Results and discussion

3.1. Optimization of CMEs preparation

To analyze the influence of PDMAEMA-*b*-PS concentration in spin-coating solutions, FESEM was introduced to investigate the morphological difference between pristine CNT membranes and fabricated CMEs. As shown in Fig. 1a, the pristine membranes are piled by CNTs with different orientations, thus forming a loose structure and irregular pores. After coated with PDMAEMA-*b*-PS and selective swelling, the morphology of electrodes is quite different from the CNT membranes. The pore size of electrodes is shrinking with the increasing concentration of spin-coated BCP solutions. After coated with only 1 wt% PDMAEMA-*b*-PS, the surface of the electrodes is significantly densified and the porosity is decreased visibly (Fig. 1b). With the increasing concentration, CNT membranes are gradually wrapped by PDMAEMA-*b*-PS and the excessive BCP attempts to form intact layers on the membrane surface (Figs. 1c-d). To further study the porosity changes, the SEM images of CNT membranes and CME-2/5 are processed by *ImageJ* [41]. As shown in Fig. S1, the total fibril area ratio of CNT membrane and CME-2/5 is ~50% and ~71%, respectively. Therefore, the porosity of the CNT membrane decreases from ~50% to ~29% after coated by 2 wt% BCP solution. TEM images further confirm the interaction between PDMAEMA-*b*-PS and CNT membranes. As shown in Fig. 1e, the graphite crystal structures of the CNT could be observed clearly in the pristine membranes [42]. However, due to the coating of PDMAEMA-*b*-PS, these structures are hard to be found in the CME-2/5 (Fig. 1f). The results in Fig. 1c and f confirm that the PDMAEMA-*b*-PS solution with a concentration of 2 wt% is enough to cover CNT membranes.

Except for the change of morphologies, the influence of PDMAEMA-*b*-PS concentration on CDI performance is also studied. As shown in Fig. 2a, after tested in the NaCl solution, all HCDI modules with CME anodes show better electrosorption capacities than the CNT membranes CDI (CCDI) module. The HCDI module with CME-2/5 anode displays the highest electrosorption capacity. As shown in the SEM images, the high-concentration BCP solution significantly reduces the porosity of the CMEs, while the low-concentration BCP solution cannot provide enough polymer to cover all CNTs. Therefore, the solution with medium concentration can wrap the CNTs better to supply enough adsorption sites and maintain the porous structure of CNT membranes to facilitate CDI processes. To select an appropriate swelling time, the CME-2/*t* samples are swollen for different times (0 h, 5 h, and 10 h) and tested as anodes in the HCDI module. As shown in Fig. 2b, all samples finish the adsorption within 60 min and the CME-2/5 samples exhibit better performance

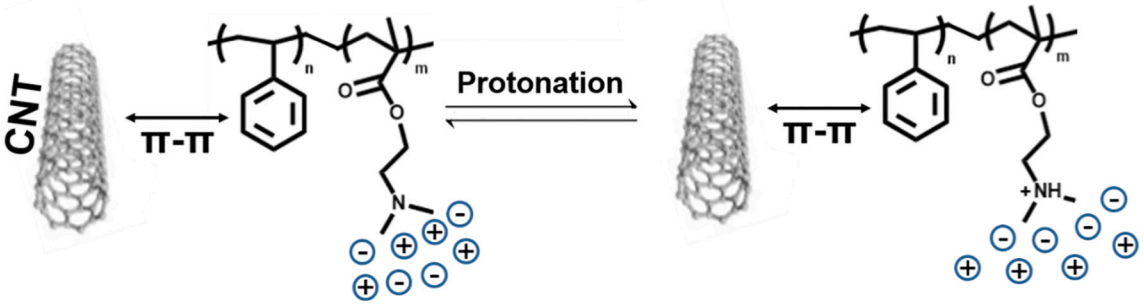

Scheme 1. The interactions between CNT membranes, BCP, and ions in the solution.

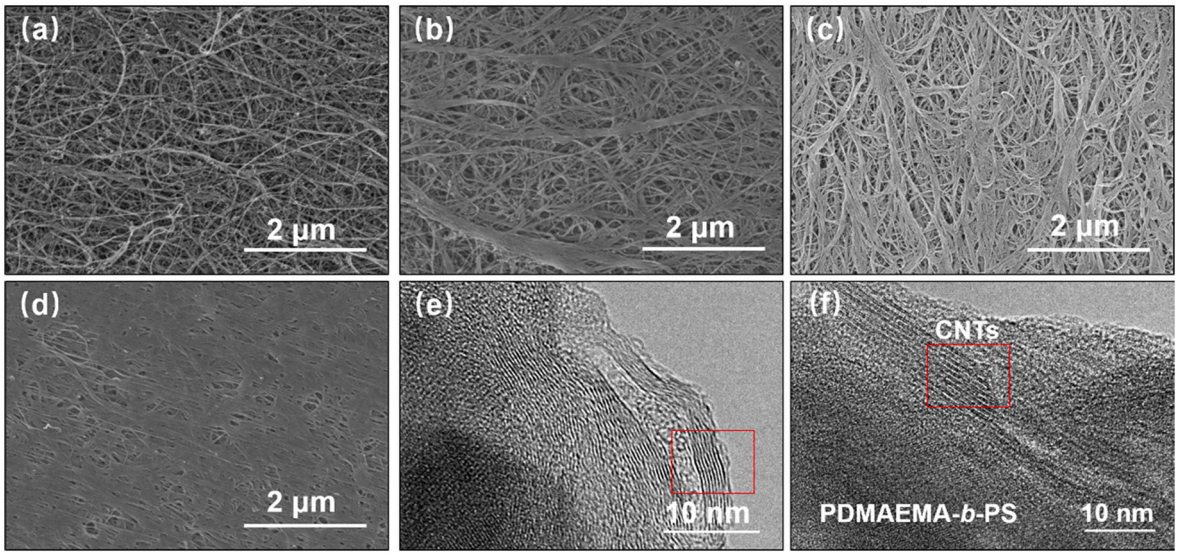

Fig. 1. FESEM images of (a) pristine CNT membranes and electrodes prepared with different PDMAEMA-*b*-PS concentrations: (b) CME-1/5, (c) CME-2/5, and (d) CME-5/5; TEM images of (e) pristine CNT membranes and (f) CME-2/5.

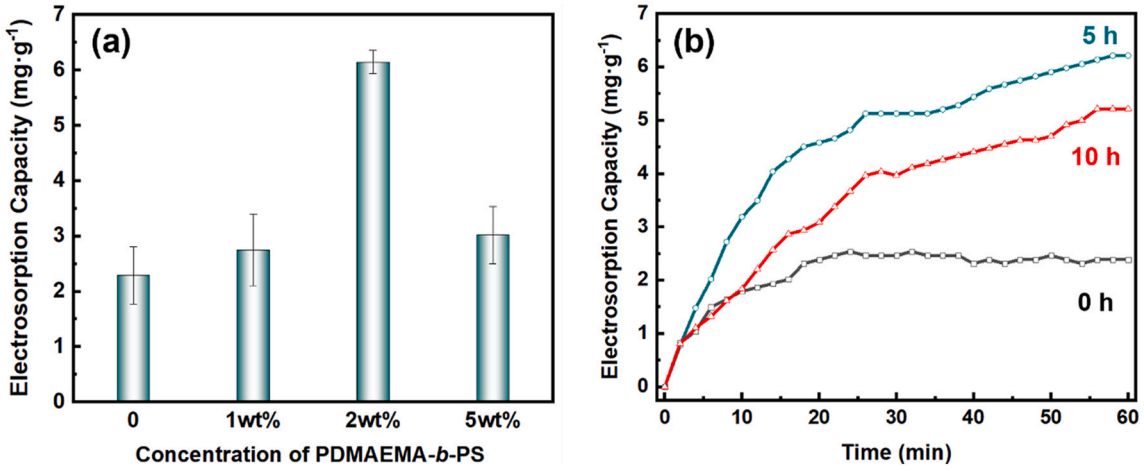

Fig. 2. The influence of (a) PDMAEMA-*b*-PS solution concentration and (b) swelling time on the electrosorption capacity of HCDI module.

than others. The selective swelling process will prompt the PDMAEMA blocks migrating to CMEs surface [39], which will provide protonated dimethylamine groups and endow the electrode with positively charged surface to adsorb anions. This result confirms that only the combination of BCPs and selective swelling can promote the electrosorption capacity of the CNT membranes.

The CDI is a wastewater treatment oriented process, the electrode with better hydrophilicity will interact with water molecules much easier. As shown in Fig. 3, the pristine CNT membranes exhibit a strong hydrophobic surface with the WCA of ~125°, which has adverse effect for the water permeation. After coated by PDMAEMA-*b*-PS, the wettability of CMEs is improved. The WCAs of CME-1/5, CME-2/5, and CME-5/5 are 112°, 105°, and 51°, respectively. The WCA of CME-2/0 samples is also investigated and its value is 116°, which is just between the pristine CNT membranes and CME-2/5. The wettability changes of different electrodes can attribute to the amount of hydrophilic groups on their surfaces. According to the XPS result, the N element on the pristine CNT membranes, 2 wt% BCP coated CNT membranes (CME-2/0) and CME-2/5 is 0%, 1.2%, and 3%, respectively (Fig. S2 and Table S1). Combining with the SEM images, the CNT membranes are gradually covered by the PDMAEMA-*b*-PS with increasing concentration, and the

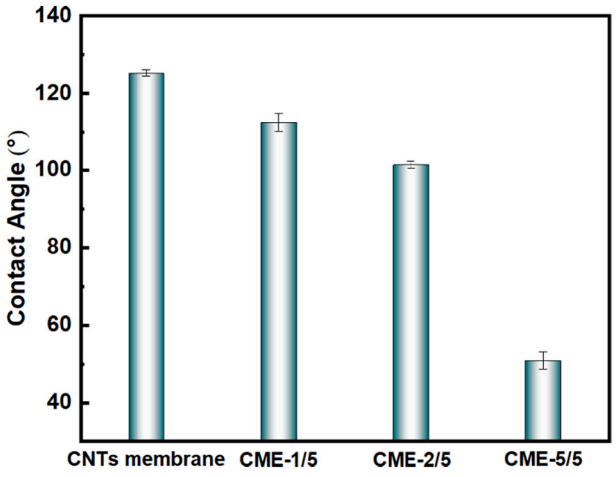

Fig. 3. Water contact angles of CNT membrane and CMEs fabricated with different PDMAEMA-*b*-PS solutions.

PDMAEMA blocks migrate to the surface after selective swelling. Therefore, the loose and hydrophobic surface is substituted by a dense and hydrophilic surface, which may improve the permeability of the electrode significantly [43]. Moreover, this result also confirms that the hydrophilicity of the CMEs can be adjusted by the coating amount of PDMAEMA-*b*-PS as well as swelling times. Based on these results, we conclude that the CMEs coated with 2 wt% PDMAEMA-*b*-PS and swollen for 5 h exhibit the best CDI performance towards NaCl solutions, and more investigations are conducted on the CME-2/5 samples for further understanding.

3.2. Chemical composition of the CME-2/5

FTIR and XPS were employed to analyze the chemical composition change of the CME-2/5. As shown in Fig. 4a, the pristine CNT membranes exhibit obvious C—H bonds stretching vibration peaks between 2900 cm^{-1} to 3000 cm^{-1}. After coated with 2 wt% PDMAEMA-*b*-PS, the peaks from CNT membranes surface are significantly weakened or even vanished due to the screen effect of BCP layer (as shown in TEM images). Instead, peaks arousing at 1728 cm^{-1} and 2770 to 2823 cm^{-1} can be attributed to the stretching vibration of C═O bonds and C—H bonds (from -$N(CH_3)_2$ groups) in the PDMAEMA blocks, respectively. These results further confirm that the CNT membranes are coated by the BCPs and the hydrophobic surface is covered by more active groups. The XPS data show that there is no nitrogen on the pristine CNTs surface, while the nitrogen content on CME-2/5 surface is 3% (Fig. 4b, Fig. S2 and Table S1). Comparing with the non-swollen CME-2/0, the nitrogen content increases from 1.2% to 3% after swelling for 5 h. The higher nitrogen content means that there are more dimethylamine groups on the CMEs surface. Based on these results, we can conclude that with appropriate PDMAEMA-*b*-PS coating amount and swelling times, the PDMAEMA blocks will migrate to the CMEs surface and provide more dimethylamine groups. Therefore, the CME-2/5 with higher nitrogen content shows better electrosorption capacity than others.

3.3. Electrochemical properties of CME-2/5

The CV test and EIS test of the CME-2/5 samples and CNT membranes were conducted in the 1 $mol{\cdot}L^{-1}$ NaCl solution. As shown in Fig. 5a, the CV curves of the pristine CNT membranes and CME-2/5 samples are shown rectangular shape under the scan rate of 10 $mV{\cdot}s^{-1}$, which confirms the typical EDL character of the electrodes. Due to the protonated PDMAEMA blocks on the CME-2/5 surface, the cation adsorption is restricted and the capacitive behavior of the CME-2/5 in the cathodic region is weakened. In contrast, the capacitive behavior of the CME-2/5 in anodic region is better than the CNT membranes [29]. This performance upgradation is also attributed to the existence of the protonated PDMAEMA blocks, which adsorb more anions by electrostatic attraction under positively charged conditions. As shown in Fig. 5b, the EIS test shows that the pristine CNT membrane has better capacitance and diffusion resistance at low frequency [44]. Meanwhile, the intercept value of CME-2/5 curve is smaller than that of the CNT membranes at high frequency (the inset of Fig. 5b), which means that the CME-2/5 has lower equivalent series resistance than the CNT membranes. Therefore, the CME-2/5 has better charge conduction capacity and low energy consumption [45,46]. These results further confirm that the CME-2/5 is more effective and suitable to be used as anodes.

3.4. The influence of module type and pH value

To select an appropriate module type for CDI processes and study its influence, three CDI modules are assembled (cathode // anode), i.e. CNT membrane // CNT membrane (CCDI) module, CNT membrane // CME-2/5 (HCDI) module, and CME-2/5 // CME-2/5 (BCP-CDI, BCDI) module. As shown in Fig. 6, the HCDI module displays the best electrosorption capacity, while the BCDI module shows the worst performance. As we mentioned before, the PDMAEMA blocks are protonated in neutral or acidic waters, thus the electrosorption capacity of the CME-2/5 towards anions is enhanced. Meanwhile, the electrosorption capacity towards cations is weakened by the electrostatic repulsion between the positively charged CME surface and Na^+ ions. Moreover, the coating of PDMAEMA-*b*-PS layers reduces the porosity of the pristine CNT membranes. Although the CME-2/5 anodes enhance the electrosorption towards anions, the CME-2/5 cathodes will repulse the cations and reduce the adsorption sites for the cations. Therefore, the BCDI module exhibits a worse electrosorption capacity than the CCDI module. By utilizing CNT membranes as cathodes and CME-2/5 as anodes in the HCDI module, the above shortcomings are averted and the advantages are fully utilized.

Due to the dimethylamine groups in the PDMAEMA-*b*-PS, the protonation degree of PDMAEMA is gradually deepened with lower pH value [47]. To confirm the influence of pH value on the CDI performance, the HCDI module was tested by NaCl solution with different pH values (4.43, 6.31, and 7.74). As shown in Fig. 7, the electrosorption capacity of the HCDI module is enhanced with decreasing pH value. When the solution turns slightly acidic, the performance of the HCDI module is improved significantly to ~6 $mg{\cdot}g^{-1}$, and this value keeps increasing with more acidic solutions. Meanwhile, the HCDI module shows a very low electrosorption capacity in slightly basic solution, which is even lower than that of the CCDI module (Fig. 7). This result illustrates that the nonprotonated PDMAEMA-*b*-PS layers are detrimental to the CDI process. To further confirm the negative influence of the nonprotonated PDMAEMA-*b*-PS, the CME-2/5 is used as cathodes in the HCDI module (inverse-HCDI, iHCDI) and tested by the basic NaCl

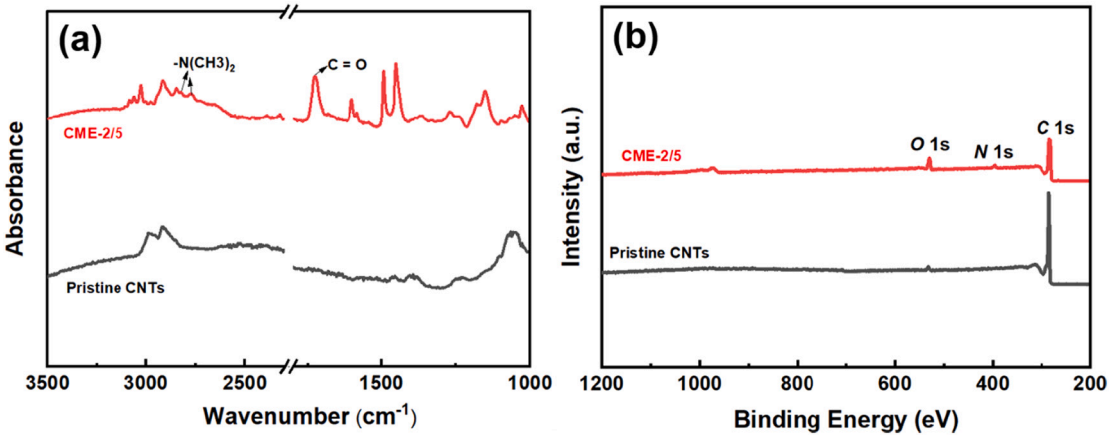

Fig. 4. (a) FTIR spectra and (b) XPS spectra of pristine CNT membranes and CME-2/5.

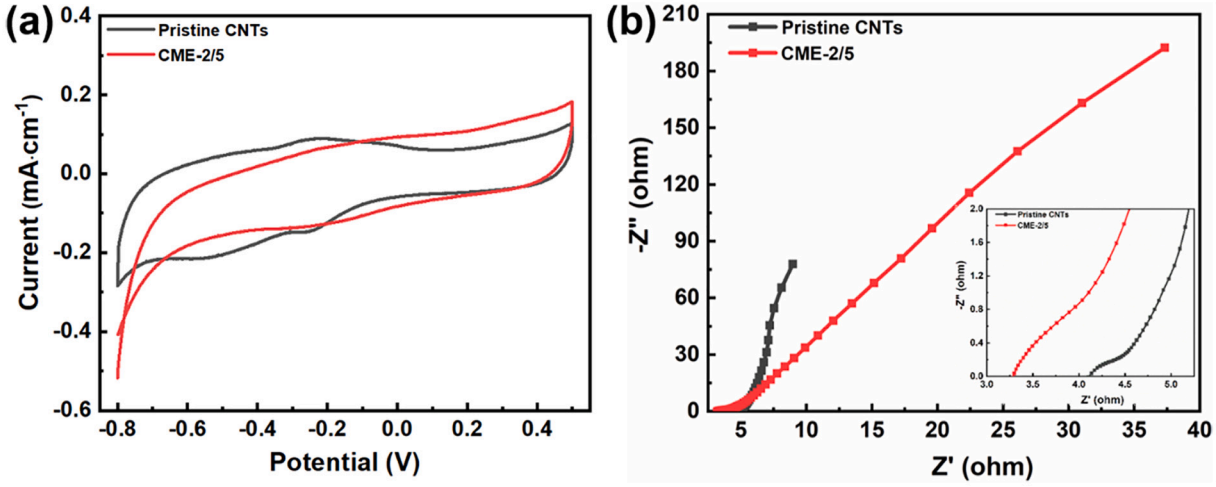

Fig. 5. (a) CV curves under scan rate of 10 mV·s^{-1} and (b) the EIS curves of pristine CNT membranes and CME-2/5, the high frequency region is enlarged and shown in the inset.

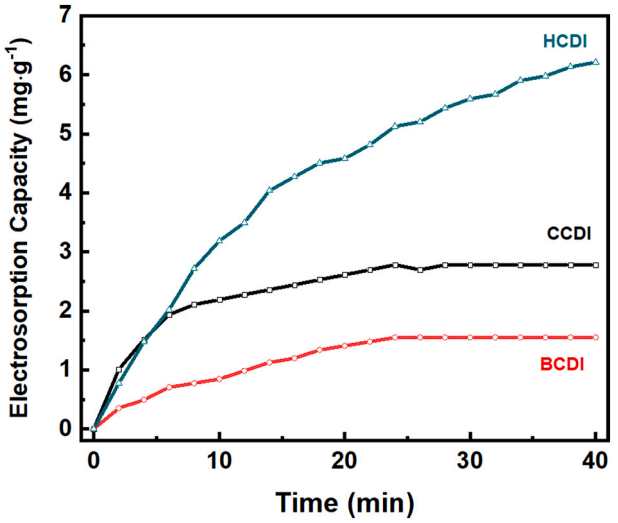

Fig. 6. Electrosorption capacity of different CDI modules.

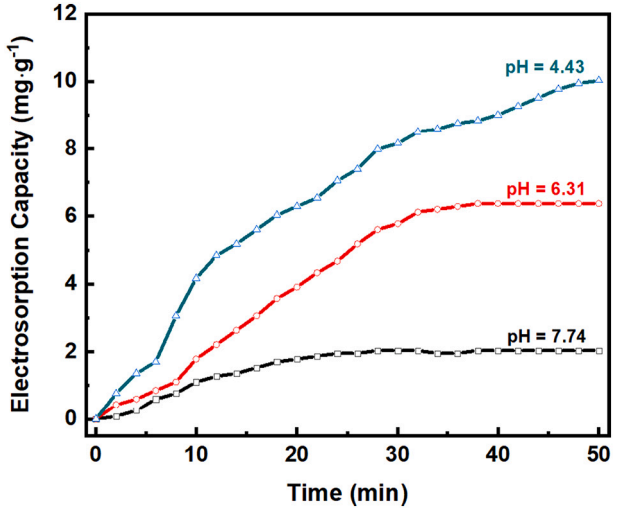

Fig. 7. Electrosorption capacity of HCDI modules with different pH values.

solution. The iHCDI module exhibits an electrosorption capacity lower than 1 mg·g^{-1} (Fig. S3), which is the worst performance among all HCDI modules in this work.

In order to explain the influence of module type, solution pH, and electrode porosity, the electrosorption capacity data are collected and summarized in Table 1. Comparing HCDI (acidic) with other tests, it can be concluded that the solution pH induced protonation is the most important impact for the CDI performance. With lower pH value, the protonation degree of PDMAEMA blocks is deepened, and more anions are adsorbed by the CME-2/5 anodes and the CDI performance of HCDI module is enhanced. This result shows that the protonated anodes can improved the performance of CDI processes and the HCDI module is very suitable for the acidic wastewater treatments. Meanwhile, the non-protonated BCP layer will impede the CDI performance, no matter the BCP layers are coated on anodes or cathodes. This phenomenon may be caused by the decrement of conductivity and porosity of the CNT membranes.

3.5. *The performance improvements of introducing CMEs*

The carbon-based electrodes are facing co-ion expulsion under high salt concentration, which may cause sever charge loss and undermine the CDI performance [48]. After coated with PDMAEMA-*b*-PS, the HCDI module exhibits improved electrosorption capacity in high-concentration NaCl solutions (Fig. 8). When the NaCl solution reaches 1000 mg·L^{-1}, the HCDI module shows an electrosorption capacity of 15 mg·g^{-1}. Moreover, the equilibrium time for the electrosorption processes is also reduced in high-concentration NaCl solutions. With higher NaCl concentrations, there are more anions adsorbed by the protonated PDMAEMA blocks on the anodes and more cations are stored by the EDL around the CNT membrane cathodes. Therefore, the HCDI module

Table 1
The performance of CDI modules with different solution pH value.

Module	pH	Porosity	Electrostatic force		Electrosorption Capacity(mg·g^{-1})[a]
			Attraction	Repulsion	
HCDI	4.43	Medium	√	×	10.0
	6.31	Medium	√	×	6.2
	7.74	Medium	×	×	2.0
CCDI	6.31	Good	×	×	2.8
BCDI	6.31	Poor	√	√	1.5
iHCDI	7.74	Medium	×	√	0.8

[a] The volume and concentration of NaCl solution are 40 mL and 100 mg·L^{-1}, respectively.

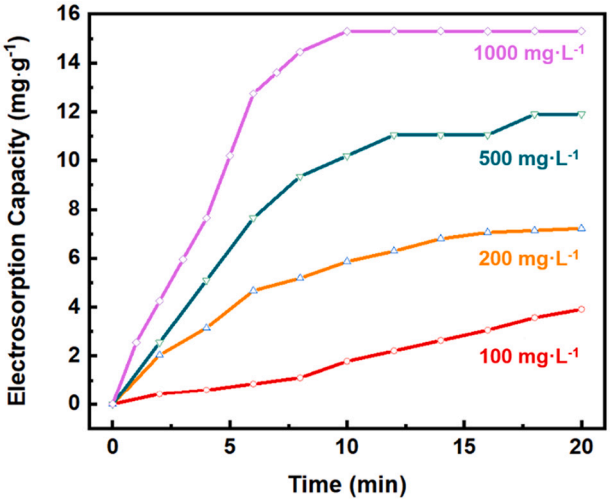

Fig. 8. Electrosorption capacity of HCDI in NaCl solutions with different concentrations.

exhibits better electrosorption capacity in the NaCl solution with high salt concentration, which confirms the co-ion expulsion is suppressed by the CME-2/5.

CDI is a promising technology for practical wastewater treatments, thus the operation stability is very important. During the CDI processes, the carbon-based anodes may react with the H_2O to release CO_2 and H^+ into the solution and gradually lose their stability. To observe whether the CME-2/5 anodes are oxidized during the CDI process, a pH meter is introduced to monitor the pH fluctuation. A 3-cycle adsorption-desorption experiment in NaCl solution (200 mg·L^{-1}) were conducted on the HCDI module under 1.2 V (charging) and 0 V (discharging), respectively. There are three possible reduction reactions on the CNT membrane cathodes, i.e. the dissolved oxygen reduces to H_2O_2, the H_2O_2 reduces to H_2O, and the H^+ ions reduces to H_2 [24]. Each of these three reactions will consume the H^+ ions in the solution. If the anodes are oxidizing during the CDI process, the H^+ ions will attain continuous supply and the pH value will keep steady. As shown in Fig. 9a, both the pH value and electrosorption capacity increase in the changing stage and decrease in the discharging stage. No obvious performance degradation is found within the 3-cycle experiment, which illustrates that there are no obvious oxidation reactions happening on the CME-2/5 and confirms that the coated PDMAEMA-*b*-PS can protect the carbon-based substrates from oxidation. During the discharge processes, the generated H_2O_2 might consume on the anodes surface and release H^+ ions into the solution, so the pH value decreases.

To further investigate the stability of the CME-2/5, another 10-cycle repeatability test was conducted. As shown in Fig. 9b, although the HCDI module exhibits electrosorption capacity fluctuation during the test, the total capacity is satisfactory and no obvious efficiency loss is found. Moreover, the CME-2/5 and pristine CNT membrane were immersed in ethanol and then sonicated for 10 min. As shown in the Fig. S4, the CNT membrane loses its original structure after sonication treatment, while the CME-2/5 can keep its structure. These results show that the coating of PDMAEMA-*b*-PS can enhance both the chemical and mechanical stabilities of the pristine CNT membranes.

3.6. Removal efficiency of HCDI module towards phosphates

Except for the NaCl, many other salts need to remove from the waters to protect the environment. Phosphorus element is one of the culprits that causes severe water eutrophication, and the phosphates originated from human activities are the main sources of phosphorus pollution. CDI has been proved as a feasible method to remove phosphates (from PO_4^{3-} to $H_2PO_4^-$) from effluents [49–51]. Moreover, the phosphate-containing wastewaters are generally acidic, therefore, our BCP coated CMEs will show satisfactory removal efficiency towards phosphates. To simulate the acidic NaH_2PO_4 solution, hydrochloric acid (HCl) was added into the NaH_2PO_4 solution (300 mg·L^{-1}) to lower down its pH to 4.21. Then 25 mL as-prepared NaH_2PO_4 solution was used as testing solution in the HCDI module (CME-2/5 used as anode) under 1.2 V. As shown in Fig. 10a, the conductivity decline of the NaH_2PO_4 solution in HCDI module is more obvious than that in the CCDI module. In order to calculate the P removal efficiency accurately, ICP is introduced to avoid the influence of Cl^- ions in the solution. According to the ICP data, the P removal efficiency of the HCDI module is 7.93 mg·g^{-1} and is ~2.7 times higher than that of the CCDI module (2.94 mg·g^{-1}), which shows that the removal efficiency of other salts can be enhanced by introducing CMEs into CDI module. To eliminate the influence of Cl^- ions and verify the effect of pH value, the pure NaH_2PO_4 solution is also tested by the HCDI module. Due to its higher pH value (5.56), the P removal efficiency of the HCDI module towards the pure NaH_2PO_4 solution is 4.67 mg·g^{-1}, which is consistent with the previous experimental results.

Considering the hydrated radius of $H_2PO_4^-$ ions (0.302 nm) and Cl^- ions (0.195 nm) [52], the much larger hydrated $H_2PO_4^-$ ions are facing stronger steric hindrance than Cl^- ions. Therefore, the coating amount of PDMAEMA-*b*-PS on the CMEs for the removal of $H_2PO_4^-$ ions needs to be reconsidered. As shown in Fig. 10b, the CME-1/5, CME-2/5, and CME-5/5 are used as anodes in the electrosorption of $H_2PO_4^-$ ions. Different from the NaCl solution, the CME-1/5 anode shows a phosphorus removal efficiency of ~10 mg·g^{-1} (~38.7 mg·g^{-1} NaH_2PO_4),

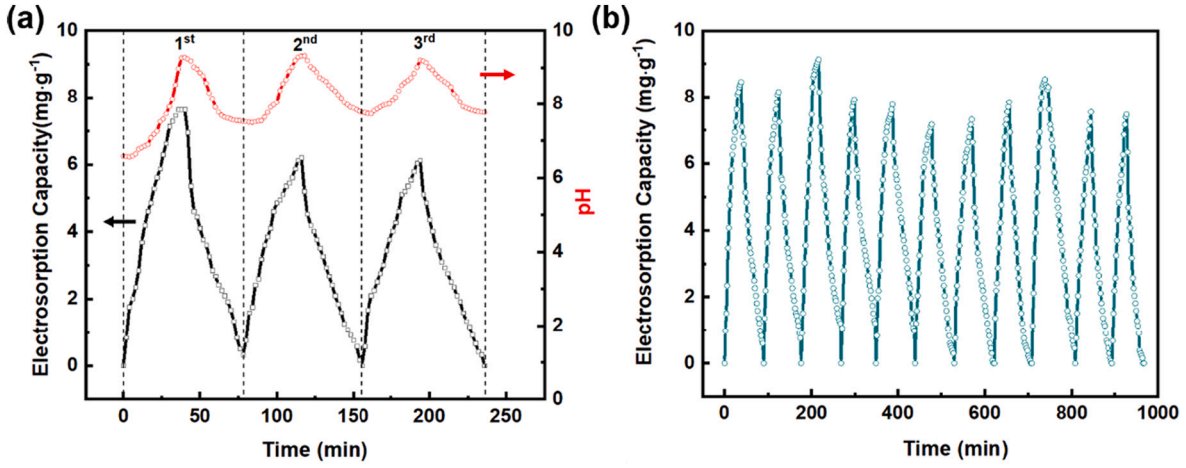

Fig. 9. (a) Changes of electrosorption capacity and pH value in a 3-cycle adsorption-desorption experiment; (b) Repeatability test of the HCDI module.

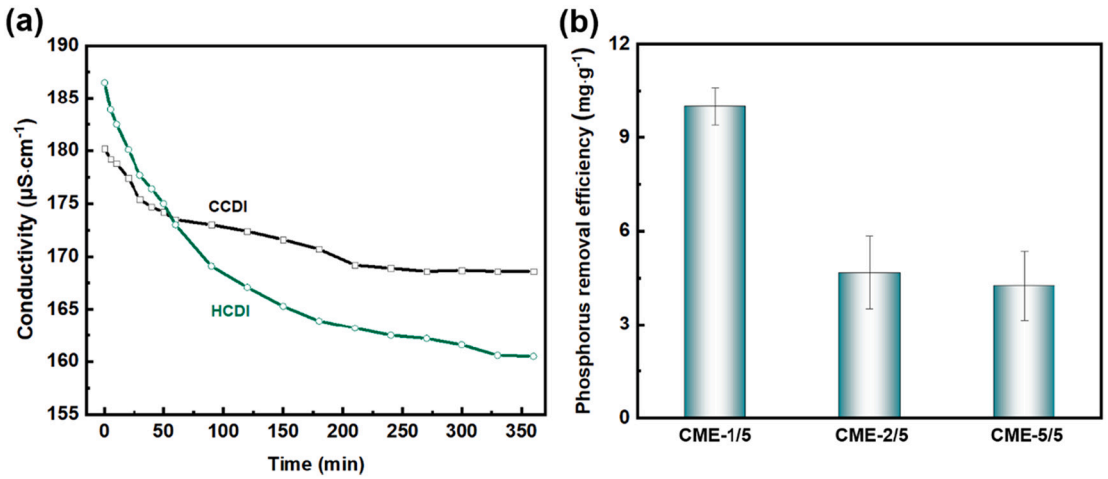

Fig. 10. (a) The conductivity changes of acidified NaH_2PO_4 solution in CCDI module and HCDI module. (b) Phosphorus removal efficiency of HCDI module with different CMEs.

which is better than other CMEs. With the increasing of PDMAEMA-*b*-PS coating amount, the steric hindrance is strengthened and the adsorbed ions hinder the subsequent adsorption, thus the electrosorption capacity of CME-2/5 is weaker than that of the CME-1/5. When the CME surface is totally wrapped by PDMAEMA-*b*-PS, the steric hindrance becomes a constant while the charge density keeps increasing, thus the steric hindrance is counterbalanced by the increment of electrostatic attraction. As a consequence, the electrosorption capacity difference between CME-2/5 and CME-5/5 is small. Moreover, this result shows good reproducibility of the CMEs, combining with the satisfactory repeatability tested in NaCl solution (Fig. 9b), the CMEs can be potential candidates for the phosphate removal by using CDI processes.

4. Conclusion

In this work, a series of PDMAEMA-*b*-PS coated CNT membranes electrodes is fabricated by a simple method and used as anodes in HCDI modules. Comparing with other anode fabrication methods, this BCP coated CNT membranes electrode can be used to deal with different salts. By utilizing the protonation characteristic of PDMAEMA-*b*-PS, the coated polymer layers enhance the CDI performance towards both NaCl and NaH_2PO_4. Experiments confirm that the initial pH of treated solution has significant influence on the performance of the HCDI module. The maximum electrosorption capacities of HCDI modules towards NaCl and NaH_2PO_4 are ~15 $mg{\cdot}g^{-1}$ and ~38.7 $mg{\cdot}g^{-1}$, respectively. Moreover, the chemical and mechanical stabilities of the pristine CNT membranes are improved by the coated PDMAEMA-*b*-PS layers, no anode oxidation can be found during the CDI processes and the frequently occurred co-ion repulsion effect is suppressed. The HCDI module can be reused for at least 10 times without obvious electrosorption capacity loss. However, the CDI performance of CMEs towards anions still requires comprehensive researches, especially the species exhibited pronounced negative effects on the environment and human activities. Considering these advantages and challenges, the PDMAEMA-*b*-PS coated anodes can be promising candidates for the hybrid CDI processes, and further researches are required to expand the application of the anodes in the desalination technology.

CRediT authorship contribution statement

Sen Xiong: Methodology, Data curation, Writing-orginal draft preparation.

Li Ren: Investigation, Validation.

Chenxu Zhang: BCP synthesis, Investigation.

Jiemei Zhou: Investigation.

Yong Wang: Conceptualization, Supervision, Writing – review & editing.

All authors have approved to the final version of the manuscript.

Declaration of competing interest

The authors declare that they have no known competing financial interests or personal relationships that could have appeared to influence the work reported in this paper.

Acknowledgements

Financial supports from National Key Research and Development Program of China (2018YFE0203502); Jiangsu Natural Science Foundation (BK20190677), and National Natural Science Foundation of China (21908096) are acknowledged.

Appendix A. Supplementary data

Supplementary data to this article can be found online at https://doi.org/10.1016/j.desal.2021.115368.

References

[1] M.A. Anderson, A.L. Cudero, J. Palma, Capacitive deionization as an electrochemical means of saving energy and delivering clean water. comparison to present desalination practices: will it compete? Electrochim. Acta 55 (2010) 3845–3856, https://doi.org/10.1016/j.electacta.2010.02.012.

[2] S. Porada, R. Zhao, A. van der Wal, V. Presser, P.M. Biesheuvel, Review on the science and technology of water desalination by capacitive deionization, Prog. Mater. Sci. 58 (2013) 1388–1442, https://doi.org/10.1016/j.pmatsci.2013.03.005.

[3] Y. Oren, Capacitive deionization (CDI) for desalination and water treatment — past, present and future (a review), Desalination 228 (2008) 10–29, https://doi.org/10.1016/j.desal.2007.08.005.

[4] X. Ma, Y.-A. Chen, K. Zhou, P.-C. Wu, C.-H. Hou, Enhanced desalination performance via mixed capacitive-faradaic ion storage using RuO2-activated carbon composite electrodes, Electrochim. Acta 295 (2019) 769–777, https://doi.org/10.1016/j.electacta.2018.10.180.

[5] S. Vafakhah, Z. Beiramzadeh, M. Saeedikhani, H.Y. Yang, A review on free-standing electrodes for energy-effective desalination: recent advances and perspectives in capacitive deionization, Desalination 493 (2020), https://doi.org/10.1016/j.desal.2020.114662.

[6] C. Zhang, D. He, J. Ma, W. Tang, T.D. Waite, Faradaic reactions in capacitive deionization (CDI) - problems and possibilities: a review, Water Res. 128 (2018) 314–330, https://doi.org/10.1016/j.watres.2017.10.024.

[7] D. He, C.E. Wong, W. Tang, P. Kovalsky, T.D. Waite, Faradaic reactions in water desalination by batch-mode capacitive deionization, Environ. Sci. Technol. Lett. 3 (2016) 222–226, https://doi.org/10.1021/acs.estlett.6b00124.

[8] I. Cohen, E. Avraham, Y. Bouhadana, A. Soffer, D. Aurbach, Long term stability of capacitive de-ionization processes for water desalination: the challenge of positive

electrodes corrosion, Electrochim. Acta 106 (2013) 91–100, https://doi.org/10.1016/j.electacta.2013.05.029.
[9] J.-B. Lee, K.-K. Park, H.-M. Eum, C.-W. Lee, Desalination of a thermal power plant wastewater by membrane capacitive deionization, Desalination 196 (2006) 125–134, https://doi.org/10.1016/j.desal.2006.01.011.
[10] Y. Liu, L. Pan, X. Xu, T. Lu, Z. Sun, D.H.C. Chua, Enhanced desalination efficiency in modified membrane capacitive deionization by introducing ion-exchange polymers in carbon nanotubes electrodes, Electrochim. Acta 130 (2014) 619–624, https://doi.org/10.1016/j.electacta.2014.03.086.
[11] J.-Y. Lee, S.-J. Seo, S.-H. Yun, S.-H. Moon, Preparation of ion exchanger layered electrodes for advanced membrane capacitive deionization (MCDI), Water Res. 45 (2011) 5375–5380, https://doi.org/10.1016/j.watres.2011.06.028.
[12] S.-I. Jeon, H.-R. Park, J.-G. Yeo, S. Yang, C.H. Cho, M.H. Han, D.K. Kim, Desalination via a new membrane capacitive deionization process utilizing flow-electrodes, Energy Environ. Sci. 6 (2013) 1471–1475, https://doi.org/10.1039/c3ee24443a.
[13] K.B. Hatzell, M.C. Hatzell, K.M. Cook, M. Boota, G.M. Housel, A. McBride, E. C. Kumbur, Y. Gogotsi, Effect of oxidation of carbon material on suspension electrodes for flow electrode capacitive deionization, Environ. Sci. Technol. 49 (2015) 3040–3047, https://doi.org/10.1021/es5055989.
[14] M. Pasta, C.D. Wessells, Y. Cui, F. La Mantia, A desalination battery, Nano Lett. 12 (2012) 839–843, https://doi.org/10.1021/nl203889e.
[15] T. Kim, C.A. Gorski, B.E. Logan, Low energy desalination using battery electrode deionization, Environ. Sci. Technol. Lett. 4 (2017) 444–449, https://doi.org/10.1021/acs.estlett.7b00392.
[16] J. Lee, S. Kim, C. Kim, J. Yoon, Hybrid capacitive deionization to enhance the desalination performance of capacitive techniques, Energy Environ. Sci. 7 (2014) 3683–3689, https://doi.org/10.1039/c4ee02378a.
[17] Z. Yue, T. Gao, H. Li, Robust synthesis of carbon@Na4Ti9O20 core-shell nanotubes for hybrid capacitive deionization with enhanced performance, Desalination 449 (2019) 69–77, https://doi.org/10.1016/j.desal.2018.10.018.
[18] J. Ai, J. Li, K. Li, F. Yu, J. Ma, Highly flexible, self-healable and conductive poly (vinyl alcohol)/Ti3C2Tx MXene film and it's application in capacitive deionization, Chem. Eng. J. 408 (2021), https://doi.org/10.1016/j.cej.2020.127256.
[19] S. Kim, J. Lee, C. Kim, J. Yoon, Na2FeP2O7 as a novel material for hybrid capacitive deionization, Electrochim. Acta 203 (2016) 265–271, https://doi.org/10.1016/j.electacta.2016.04.056.
[20] Y. Li, Z. Ding, J. Li, J. Li, T. Lu, L. Pan, Highly efficient and stable desalination via novel hybrid capacitive deionization with redox-active polyimide cathode, Desalination 469 (2019), https://doi.org/10.1016/j.desal.2019.114098.
[21] Y. Li, Z. Ding, X. Zhang, J. Li, X. Liu, T. Lu, Y. Yao, L. Pan, Novel hybrid capacitive deionization constructed by a redox-active covalent organic framework and its derived porous carbon for highly efficient desalination, J. Mater. Chem. A 7 (2019) 25305–25313, https://doi.org/10.1039/c9ta07344b.
[22] J. Chang, K. Tang, H. Cao, Z. Zhao, C. Su, Y. Li, F. Duan, Y. Sheng, Application of anion exchange membrane and the effect of its properties on asymmetric membrane capacitive deionization, Sep. Purif. Technol. 207 (2018) 387–395, https://doi.org/10.1016/j.seppur.2018.06.063.
[23] Q. Qiu, J.-H. Ch, Y.-W. Choi, J.-H. Choi, J. Shin, Y.-S. Lee, Preparation of polyethylene membranes filled with crosslinked sulfonated polystyrene for cation exchange and transport in membrane capacitive deionization process, Desalination 417 (2017) 87–93, https://doi.org/10.1016/j.desal.2017.05.008.
[24] Y. Li, Z. Ding, J. Li, K. Wang, T. Lu, L. Pan, Novel membrane-free hybrid capacitive deionization with a radical polymer anode for stable desalination, Desalination 481 (2020), https://doi.org/10.1016/j.desal.2020.114379.
[25] D.-H. Nam, K.-S. Choi, Bismuth as a new chloride-storage electrode enabling the construction of a practical high capacity desalination battery, J. Am. Chem. Soc. 139 (2017) 11055–11063, https://doi.org/10.1021/jacs.7b01119.
[26] M.R. Vengatesan, I.F.F. Darawsheh, B. Govindan, E. Alhseinat, F. Banat, Ag-cu bimetallic nanoparticle decorated graphene nanocomposite as an effective anode material for hybrid capacitive deionization (HCDI) system, Electrochim. Acta 297 (2019) 1052–1062, https://doi.org/10.1016/j.electacta.2018.12.004.
[27] H. Yoon, J. Lee, S. Kim, J. Yoon, Hybrid capacitive deionization with ag coated carbon composite electrode, Desalination 422 (2017) 42–48, https://doi.org/10.1016/j.desal.2017.08.010.
[28] Y. Shi, X. Zhou, G. Yu, Material and structural design of novel binder systems for high-energy, high-power lithium-ion batteries, Acc. Chem. Res. 50 (2017) 2642–2652, https://doi.org/10.1021/acs.accounts.7b00402.
[29] X. Gao, A. Omosebi, N. Holubowitch, A. Liu, K. Ruh, J. Landon, K. Liu, Polymer-coated composite anodes for efficient and stable capacitive deionization, Desalination 399 (2016) 16–20, https://doi.org/10.1016/j.desal.2016.08.006.
[30] Y. Wang, L. Zhang, Y. Wu, S. Xu, J. Wang, Polypyrrole/carbon nanotube composites as cathode material for performance enhancing of capacitive deionization technology, Desalination 354 (2014) 62–67, https://doi.org/10.1016/j.desal.2014.09.021.
[31] P. Nie, J. Yan, G. Zhu, J. Liu, Inverted hybrid-capacitive deionization with polyaniline nanotubes doped activated carbon as an anode, Electrochim. Acta 339 (2020), https://doi.org/10.1016/j.electacta.2020.135920.
[32] C. Yan, L. Zou, R. Short, Polyaniline-modified activated carbon electrodes for capacitive deionisation, Desalination 333 (2014) 101–106, https://doi.org/10.1016/j.desal.2013.11.032.
[33] H. Kong, M. Yang, Y. Miao, X. Zhao, Polypyrrole as a novel chloride-storage electrode for seawater desalination, Energy Technol. 7 (2019), https://doi.org/10.1002/ente.201900835.
[34] Y. Kitao, Y. Kimura, H. Asamoto, H. Minamisawa, K. Yamada, Enhancement of Cr (VI) ion adsorption by two-step grafting of methacrylamide (MAAm) and 2-(dimethylamino)ethyl methacrylate (DMAEMA) onto polyethylene plate, Environ. Technol. (2020), https://doi.org/10.1080/09593330.2020.1864481.
[35] A. Bratek-Skicki, Design of ultra-thin PEO/PDMAEMA polymer coatings for tunable protein adsorption, Polymers 12 (2020), https://doi.org/10.3390/polym12030660.
[36] J. Feng, S. Xiong, L. Ren, Y. Wang, Atomic layer deposition of TiO2 on carbon-nanotubes membrane for capacitive deionization removal of chromium from water, Chin. J. Chem. Eng. (2021), https://doi.org/10.1016/j.cjche.2021.05.014.
[37] J. Feng, S. Xiong, Y. Wang, Atomic layer deposition of TiO2 on carbon-nanotube membranes for enhanced capacitive deionization, Sep. Purif. Technol. 213 (2019) 70–77, https://doi.org/10.1016/j.seppur.2018.12.026.
[38] J. Feng, S. Xiong, Z. Wang, Z. Cui, S.-P. Sun, Y. Wang, Atomic layer deposition of metal oxides on carbon nanotube fabrics for robust, hydrophilic ultrafiltration membranes, J. Membr. Sci. 550 (2018) 246–253, https://doi.org/10.1016/j.memsci.2018.01.003.
[39] C. Zhang, C. Yin, Y. Wang, J. Zhou, Y. Wang, Simultaneous zwitterionization and selective swelling-induced pore generation of block copolymers for antifouling ultrafiltration membranes, J. Membr. Sci. 599 (2020), 117833, https://doi.org/10.1016/j.memsci.2020.117833.
[40] X. Yao, J. Li, L. Kong, Y. Wang, Surface functionalization of carbon nanotubes by direct encapsulation with varying dosages of amphiphilic block copolymers, Nanotechnology 26 (2015), 325601, https://doi.org/10.1088/0957-4484/26/32/325601.
[41] C.A. Schneider, W.S. Rasband, K.W. Eliceiri, NIH image to ImageJ: 25 years of image analysis, Nat. Methods 9 (2012) 671–675, https://doi.org/10.1038/nmeth.2089.
[42] S.C. Lyu, H.W. Kim, S.J. Kim, J.W. Park, C.J. Lee, Synthesis and crystallinity of carbon nanotubes produced by a vapor-phase growth method, Appl. Phys. A Mater. Sci. Process. 79 (2004) 697–700, https://doi.org/10.1007/s00339-003-2252-z.
[43] S. Xiong, X. Jia, K. Mi, Y. Wang, Upgrading polytetrafluoroethylene hollow-fiber membranes by CFD-optimized atomic layer deposition, J. Membr. Sci. 617 (2021), https://doi.org/10.1016/j.memsci.2020.118610.
[44] X. Min, X. Hu, X. Li, H. Wang, W. Yang, Synergistic effect of nitrogen, sulfur-codoping on porous carbon nanosheets as highly efficient electrodes for capacitive deionization, J. Colloid Interf. Sci. 550 (2019) 147–158, https://doi.org/10.1016/j.jcis.2019.04.082.
[45] M. Li, H.G. Park, Pseudocapacitive coating for effective capacitive deionization, ACS Appl. Mater. Interfaces 10 (2018) 2442–2450, https://doi.org/10.1021/acsami.7b14643.
[46] Z. Wang, T. Yan, G. Chen, L. Shi, D. Zhang, High salt removal capacity of metal-organic gel derived porous carbon for capacitive deionization, ACS Sustain. Chem. Eng. 5 (2017) 11637–11644, https://doi.org/10.1021/acssuschemeng.7b03015.
[47] F.G. Santos, L.C. Bonkovoski, F.P. Garcia, T.S.P. Cellet, M.A. Witt, C.V. Nakamura, A.F. Rubira, E.C. Muniz, Antibacterial performance of a PCL–PDMAEMA blend nanofiber-based scaffold enhanced with immobilized silver nanoparticles, ACS Appl. Mater. Interfaces 9 (2017) 9304–9314, https://doi.org/10.1021/acsami.6b14411.
[48] Y. Li, Z. Ding, J. Li, K. Wang, T. Lu, L. Pan, Novel membrane-free hybrid capacitive deionization with a radical polymer anode for stable desalination, Desalination 481 (2020), 114379, https://doi.org/10.1016/j.desal.2020.114379.
[49] X. Huang, D. He, W. Tang, P. Kovalsky, T.D. Waite, Investigation of pH-dependent phosphate removal from wastewaters by membrane capacitive deionization (MCDI), Environ. Sci.: Water Res. 3 (2017) 875–882, https://doi.org/10.1039/c7ew00138j.
[50] C. Zhang, M. Wang, W. Xiao, J. Ma, J. Sun, H. Mo, T.D. Waite, Phosphate selective recovery by magnetic iron oxide impregnated carbon flow-electrode capacitive deionization (FCDI), Water Res. 189 (2021), https://doi.org/10.1016/j.watres.2020.116653.
[51] X. Hong, E. Zhu, Z. Ye, K.S. Hui, K.N. Hui, Enhanced phosphate removal under an electric field via multiple mechanisms on MgAl-LDHs/AC composite electrode, J. Electroanal. Chem. 836 (2019) 16–23, https://doi.org/10.1016/j.jelechem.2019.01.046.
[52] M.Y. Kiriukhin, K.D. Collins, Dynamic hydration numbers for biologically important ions, Biophys. Chem. 99 (2002) 155–168, https://doi.org/10.1016/S0301-4622(02)00153-9.